JOURNAL OF MATERIALS SCIENCE 33 (1998) 487–496

Scanning tunnelling microscopy and transmission electron microscopy study of ultrafine structure and surface relief of bainite in a Cu–Zn–Al alloy

CHUN-MING LI*‡, HONG-SHENG FANG‡, ZHI-GANG YANG‡, XIANG-ZHENG BO‡, JIA-JUN WANG‡, YAN-KANG ZHENG‡
Departments of Modern Applied Physics and ‡Materials Science and Engineering, Tsinghua University, Beijing 100084, People's Republic of China

The fine structure of bainite (α_1 plate) in a Cu–25.9 wt% Zn–4.0 wt% Al–0.1 wt% Re alloy has been studied by scanning tunnelling microscopy (STM) and transmission electron microscopy (TEM). The experimental results demonstrated that bainite plates are composed of subplates, and the subplates are composed of subunits. STM investigation shows that the surface relief with a bainite plate is composed of groups of small reliefs which correspond to subplates and subunits. The relief arising from the formation of bainite is tent like, which is different from that with martensite. Ledges exist on the broad faces of the subunit, indicating that it grows by a ledgewise mechanism. Three types of nucleation of the subunits were observed under TEM: face to face, edge to edge and edge to face. Based on the experimental results concerning the ultrafine structure and surface relief accompanying bainite, the sympathetic nucleation–ledgewise growth mechanism of bainite is proposed.

1. Introduction

The bainite transformation mechanism has been controversial for more than half a century ever since the first investigation in steel by Robertson as it involves both diffusional and shear characteristics [1–4]. In the 1950s, Garwood [5, 6] found that this type of transformation occurs also in non-ferrous substitutional Cu–Zn alloys. Similarly, the transformation in this kind of alloy takes on a dual nature such as a C-curve type of incubation kinetics which indicates a thermally activated process [5, 7], the crystallography and the surface relief effect resembling those of the low-temperature martensites [8, 9], as well as a composition adjustment implying that long-range substitutional diffusion is required to achieve equilibrium [10–14]. These complicated behaviours led to considerable controversy as to whether bainite forms by a shear mechanism or long-range diffusion.

As the transformation mechanism of bainite is very closely related to its fine structure, up to now, almost all the research studies concerning this transformation have been made with the most powerful analytical tools in the history of investigation such as scanning electron microscopy (SEM) and transmission electron microscopy (TEM). So far, bainite in Cu-based alloys were found to be plate-like under SEM and TEM. As for the finer interior structure, it remains unknown because of the resolution ability of the experimental instruments employed. So, it is imperative to introduce a new analysis microscopy with a more powerful resolution ability so as to reveal the ultrafine structure of bainites.

Scanning tunnelling microscopy is a new surface analysis microscopy which was developed successfully in 1982 by Binnig and Rohrer [15]. To date, STM has been widely used in the fields of surface science, materials science, life science, etc., as it has a high resolution ability (its vertical resolution ability can reach 0.01 nm while the lateral resolution ability can reach 0.1 nm), shows the three-dimensional images of objects in true space, can observe the local area surface structure of single atom layer, operates under different conditions such as vacuum, air and ambient temperature and also does not result in any sample destruction [16]. The present authors have successfully observed the ultrafine structure of lower bainite in steels with the aid of STM and revealed the subsubunit structure which has not been reported before [17].

In order to provide further evidence in resolving the controversy about the transformation of bainite, this

* *Present address*: Department of Mechanical Engineering, Shizuoka Institute of Science and Technology, Toyosawa 2200-2, Fukuroi-City, Shizuoka 437, Japan.

0022–2461

paper deals with the interior and interface boundary structure of bainite in Cu–Zn–Al alloy by means of STM and TEM. Similar to the ultrafine structure of bainite in steels, α_1 plate in Cu–Zn–Al alloy was also found to consist of subplates, and the subplates to consist of subunits. Also, the surface relief obtained with bainite and martensite were also studied by STM. The results indicated that the surface relief with martensite is of an invariant plane-strain (IPS) type and that with bainite is tent like. According to the present results, a transformation mechanism, namely, the sympathetic nucleation–ledgewise growth mechanism, is discussed.

2. Experimental procedure

Specimens of Cu–25.9 wt% Zn–4.0 wt% Al–0.1 wt% Re were homogenized at 850 °C for 12 h, solutionized for 3 min at 750 °C and then isothermally reacted at moderate temperatures for a short time to form α_1 plates. STM specimens were prepared by polishing and etching the samples after they had been mechanically ground. The etching reagent is 5 g of $FeCl_3$ + 2 ml of HCl + 100 ml of C_2H_5OH. STM operation was performed in air at ambient temperature under a constant-tunnelling-current mode (as shown in Fig. 1) with a bias voltage of 200 mV and tunnelling currents of 0.5 and 0.9 nA while the specimen was covered with a layer of glycerol so as to keep the freshly etched surface from oxidizing. The tip made of tungsten filament was electrolytically etched in a NaOH solution and connected to ground when in operation. The specimen of surface reliefs were electropolished in an orthophosphoric acid (70 vol%) water solution and quenched into liquid nitrogen to obtain martensite accompanied by surface relief, or austempered at 350 °C for 30 min in a vacuum furnace (10^{-3} Pa) to obtain surface relief with bainite. Foil specimens for TEM were made from those which had been observed under STM. Having been ground to a thickness of 50 μm, they were electrolytically thinned at − 30 °C by a twin-jet technique, conducted with a potential of 70 V and a current of 30 mA in a solution of 5% $HClO_4$ + 95% C_2H_5OH. Finally, ion beam thinning of the thin foils was introduced to provide better thin regions. TEM analysis was carried out in a H-800 microscope operating at 200 kV.

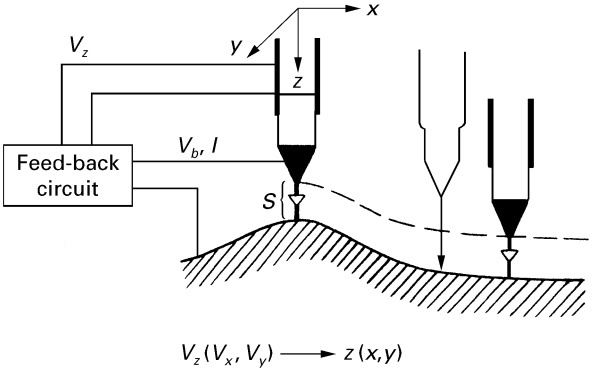

Figure 1 Schematic drawing of STM scanning in a constant-current mode where S is the distance between the tip and specimen, I and V_b are the tunnelling current and biased voltage, respectively, and V_z is the feedback voltage controlling the movement of tip in the z direction.

3. Experimental results

3.1. Bainites in Cu–Zn–Al alloy under scanning tunnelling microscopy

Fig. 2 is an optical micrograph of the specimen, exhibiting typical bainites with an obtuse angle of "V" shape lying on the white matrix (B2 phase), as illustrated by the arrows. The length and width of these bainite plates are 10 μm and 0.2–0.8 μm, respectively. The scanning electron micrograph of the specimen is shown in Fig. 3. It can be seen that the interfacial boundary between the bainite and matrix is not even (see the arrows), as if the plate were discontinuous. As the resolution ability of SEM is very limited, the fine structure of the bainite cannot be distinguished.

The etched surface microstructure of the specimen under STM is given in Fig. 4. It should be pointed out that the scanning range and resolution ability of STM are the two contradictory key elements which have important effects on the quality of image. If the scanning range is too small, the images obtained through STM will also be restricted in a tiny area of the specimen and cannot be linked up continuously with the optical and scanning electron micrographs. As it is

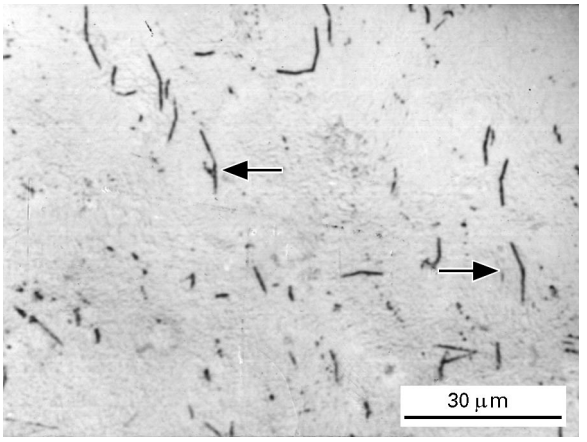

Figure 2 Optical micrograph of the specimen (350 °C; 5 s).

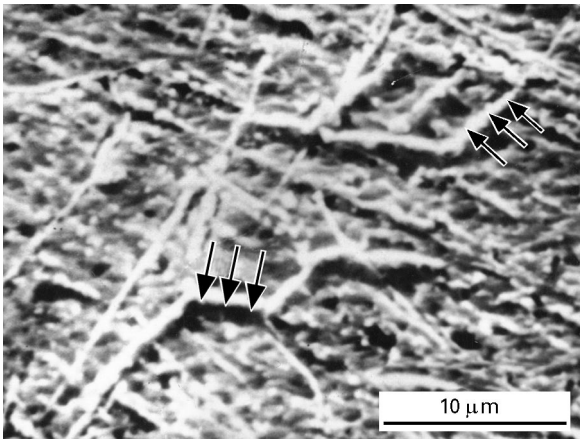

Figure 3 Scanning electron micrograph of the specimen (350 °C; 5 s).

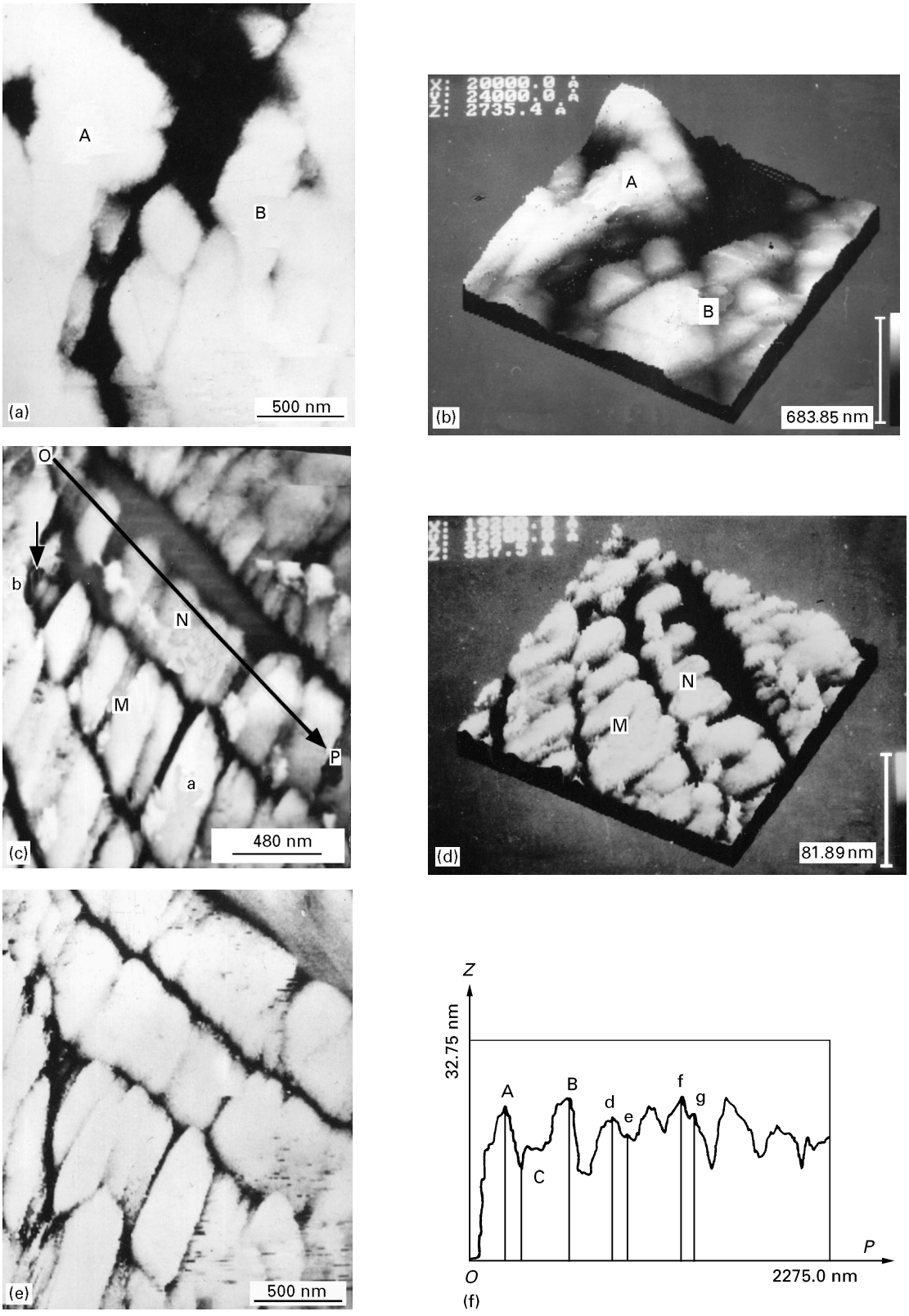

Figure 4(a)–(e) Scanning tunnelling micrographs of the specimens: (a) corner part of bainite (350 °C; 5 s), with $V = 200.0$ mV, $I = 0.90$ nA, $x = 2000.00$ nm, $y = 2400.00$ nm and $Z = 273.54$ nm; (b) three-dimensional morphology of (a); (c) front part of a bainite plate (306 °C; 45 s), with $V = 200.0$ mV, $I = 0.50$ nA, $x = 1920.00$ nm, $y = 1920.00$ nm and $Z = 32.75$ nm; (d) three-dimensional morphology of (c); (e) middle part of a bainite plate (306 °C; 45 s), with $V = 200.0$ mV, $I = 0.50$ mΛ, $x = 2000.00$ nm, $y = 2400.00$ nm and $z = 46.13$ nm. (f) Surface profile of the bainite N in (c).

the first time that the bainitic structure in Cu-based alloys by STM has been investigated, the structure on such tiny images obtained from the specimen cannot be distinguished if the scanning range is too narrow. On the other hand, if the scanning range is too large, then the resolution ability will decrease correspondingly and cannot provide the fine structure of the specimen. Considering the above contrary factors and the present conditions in manufacturing the piezoid, the scanning range involved in this paper is

2000 nm × 2400 nm and 1920 nm × 1920 nm, i.e., the tip scanned 2000 nm and 1920 nm along the X direction and 2400 nm and 1920 nm along the Y direction, respectively. 200 data were collected in each line along the X direction and 200 lines were adopted along the Y direction in each image. So the corresponding point resolution power along the X and Y directions is 10, 9.6 nm and 12, 9.6 nm. These ranges proved to be appropriate for STM observation.

Similar to the results in Fig. 2 and Fig. 3, the morphology of the structures in Fig. 4 is also plate like. In Fig. 4a, A and B are two bainite plates with their three-dimensional morphologies in Fig. 4b in which A refers to a corner part of a plate. M and N in Fig. 4c are the tips of two bainite subplates and Fig. 4d shows their three-dimensional morphologies. Fig. 4e corresponds to the middle part of the bainite plates. The experimental results show that all the bainite plates are 0.2–0.8 μm wide, in agreement with that under the results obtained by optical microscopy, scanning electron microscopy (SEM) and TEM and that they have similar morphologies. As there is only one phase (bainite) in the matrix, the structure observed by STM in Fig. 4 is bainite exactly.

3.2. Subunit of bainite in Cu–Zn–Al alloy

3.2.1. Scanning tunnelling microscopy observation

Up to now, the delicate structure of bainite plate in Cu–Zn–Al alloy has never been reported because of the resolution limit of analytical tools. From Fig. 4a–e, it can be seen that the bainite plate is composed of subplates and that the subplates consist of small subunits. It was also found that there exists a small degree of roughness on their surface. In order to detect the surface corrugation, the bainite N in Fig. 4c was sectioned along the OP direction. The result is illustrated in Fig. 4f, in which the maximum height of coordinate Z is 32.75 nm. This is the maximum depth of the etched specimen surface detected. It reveals that hollows exist between subunits, as shown by the valley zone of the curve. This indicates that the subunit is the real fine structure of bainite plate, as the regular hollows are the result of etching. A potential difference exists between the subunit and its boundary area. The boundary, as the electrochemical anode, was etched out. In Fig. 4f, the lowest point C between subunits A and B is about 9.2 nm lower than A and B. This is the maximum depth between the subunit and the boundary of two subunits.

It is apparent from Fig. 4 that the subunits decrease progressively in size along the growth direction of bainite plate and range regularly in accordance with the growth sequence. The largest subunit is near the original part of the plate which is about 800 nm × 300 nm while the smallest subunit is at the tip of the plate with a size of about 60 nm × 60 nm, as shown by A and B in Fig. 4c. In addition, the subunits are of regular shape and range in order, which implies that they have a definite habit plane and precipitate one by one; this will be discussed later in this paper.

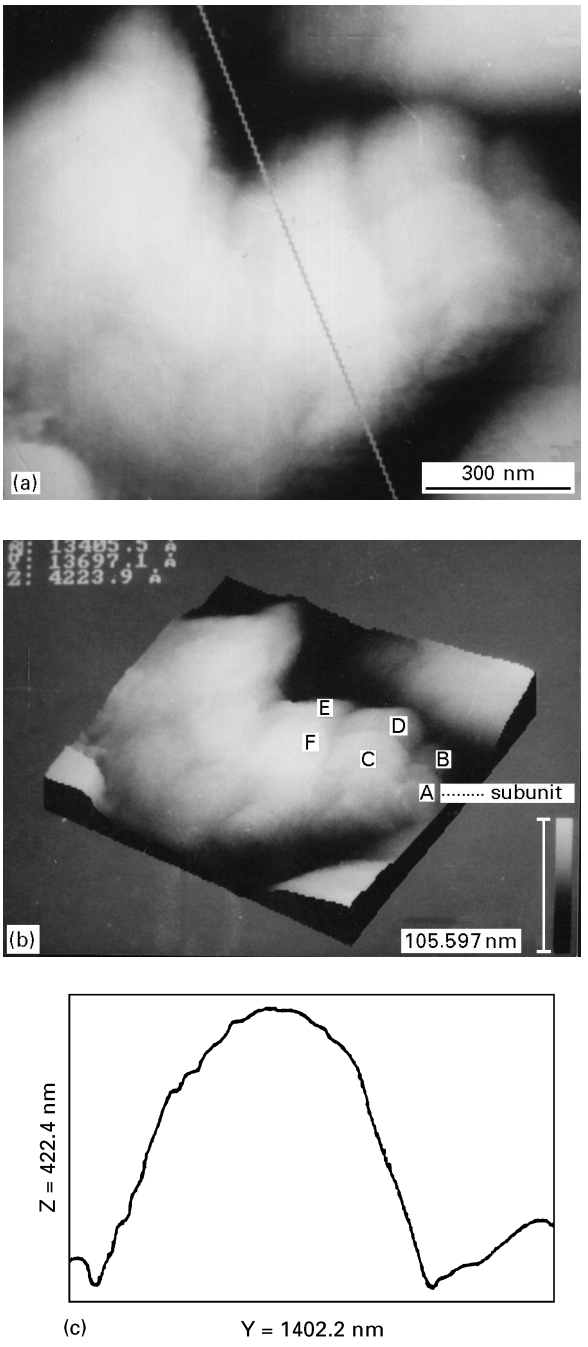

Figure 5 Surface relief with bainite obtained by STM in air in ambient conditions (350 °C; 30 min); (a) two-dimensional image; (b) three-dimensional image of (a); (c) profile corresponding to the line in (a) showing the height differences of relief with bainite. (The scales for height and width are different.)

3.2.2. Surface relief

In order to confirm the experimental results concerning the subunit of bainite obtained from the etched specimen surfaces, experiments were also carried out on fresh surface reliefs produced on the polished specimen heat treated in a high vacuum.

Fig. 5 shows the surface relief accompanying bainitic transformation. The two bainite plates are coupled in a typical shape of "V" with an obtuse angle. It is very clear that the substructure exists in the relief as indicated by A, B, C, D, E and F in Fig. 5b, which are referred to as subunits. From the profile line in Fig. 5c, it can be seen that the relief is not of IPS type but of "tent-like" shape, with a height of 0.4 μm. As the

profile arises from the total contribution of subunits, it has no physical sense due to the interaction and interference between the subunits and cannot delineate the formation mechanism of bainite. Taking into account this consideration, a single surface relief produced by a unique subunit must be investigated in order to reflect the nature of the bainitic transformation.

The surface relief at the tip of the α_1 plate is demonstrated in Fig. 6. The shape of the surface relief with bainite is also tent like and not of IPS type. From Fig. 6a, three small plates (labelled P, Q and R) in the relief with a width of 0.2–0.3 μm can be distinguished, corresponding to the subplates of bainite. The subplates are composed of smaller units in the longitudinal direction, corresponding to subunits (labelled E, F, G, H, I and J). This can also be seen from Fig. 6b. The profile line has three sawteeth; each corresponds to a subplate. The height difference between subplates is about 10 nm. From Fig. 6c, the sawteeth in profile C correspond to subunits of subplate Q. From these experiments, we can see that the surface relief with all the bainite is actually groups of small reliefs raised by the subplates and subunits. As mentioned above, it is imperative to observe the relief with a single subunit. The result can be seen from profile D in Fig. 6d. Again, the shape of a single relief with a subunit is also shown to be tent like rather than of IPS type. The size of the subunit is about 300 nm × 100 nm, which is the same order as that observed under STM.

3.2.3. Transmission electron microscopy observation

On the basis of the discovery of the subunit by STM, TEM observation was also carried out in order to confirm the existence and interior structure of the subunits. Fig. 7 shows a transmission electron micrograph of bainite imaged under nearly the double-beam condition. Fig. 7b is the dark field micrograph imaged by the $(130)_{\alpha_1}$ diffraction in Fig. 7c which demonstrates clearly that the bainite plate consists of subunits. It is apparent that the size of the largest subunit A is about 1100 nm × 800 nm, and the size of subunit B at the tip is about 600 nm × 500 nm; these are also the same order of size as those observed by STM. Another set of diffraction pattern can be indexed as the $[03\bar{1}]$ crystal axis of the matrix. Fig. 7d is the indexing result corresponding to Fig. 7c.

Fig. 8 shows the morphology of bainite in the specimen heat treated at 250 °C for 6 min. Subunits can also be observed. The size of the largest is 200 nm × 80 nm and the size of B is 60 nm × 60 nm, as indicated in Fig. 8a.

It is revealed in Fig. 8 that an array of ledges exists on the subunit at the tip of the bainite with a height of about 8 nm, as shown by the arrow. This indicates that subunits grow by a ledgewise mechanism. In a previous study, Chattopadhyay and Aaronson [18] found that α_1 plates are fully coherent and also free of internal structure during the earliest observed stage of their growth. Both interface boundary structure and thickening kinetics were shown to be inconsistent with

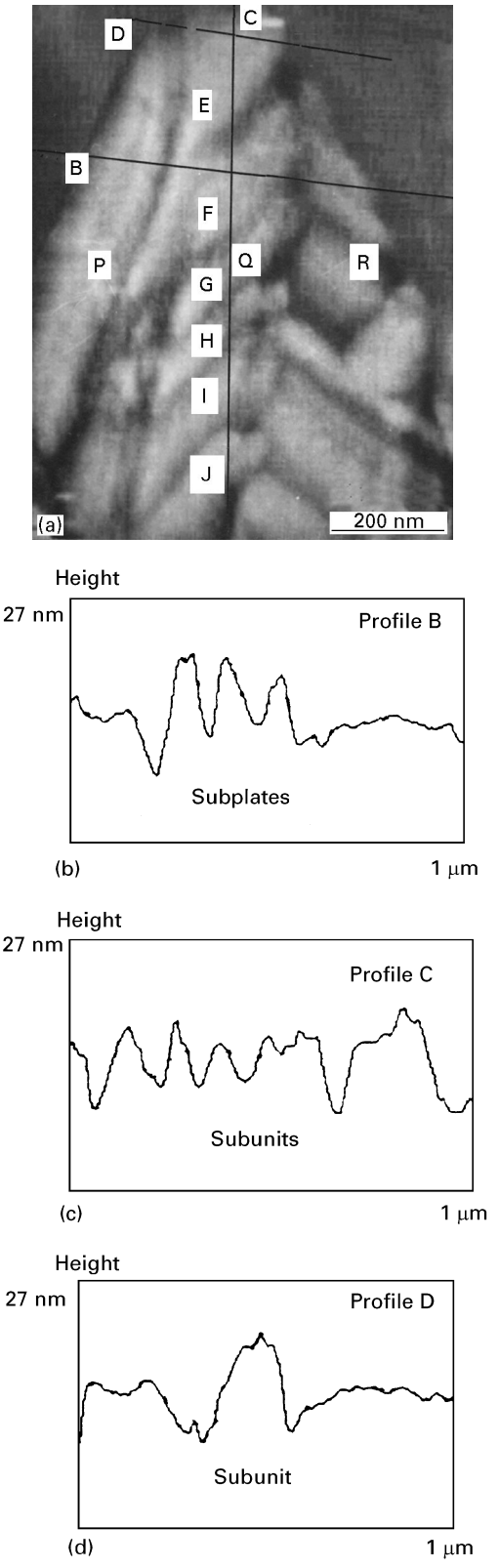

Figure 6 (a) Two-dimensional image of the surface relief with a tip of bainite taken by STM in air in ambient conditions (350 °C; 30 min); (b)–(d), the profiles corresponding to the lines B–D in (a), showing the height differences of relief with bainite. (The scales for height and width are different).

various shear mechanisms of growth but to fit comfortably into the framework provided by diffusion-controlled ledgewise thickening.

The interface boundary structure of bainite plate in Cu–Zn–Al alloys had also been observed by the present authors. It was found that three-dimensional

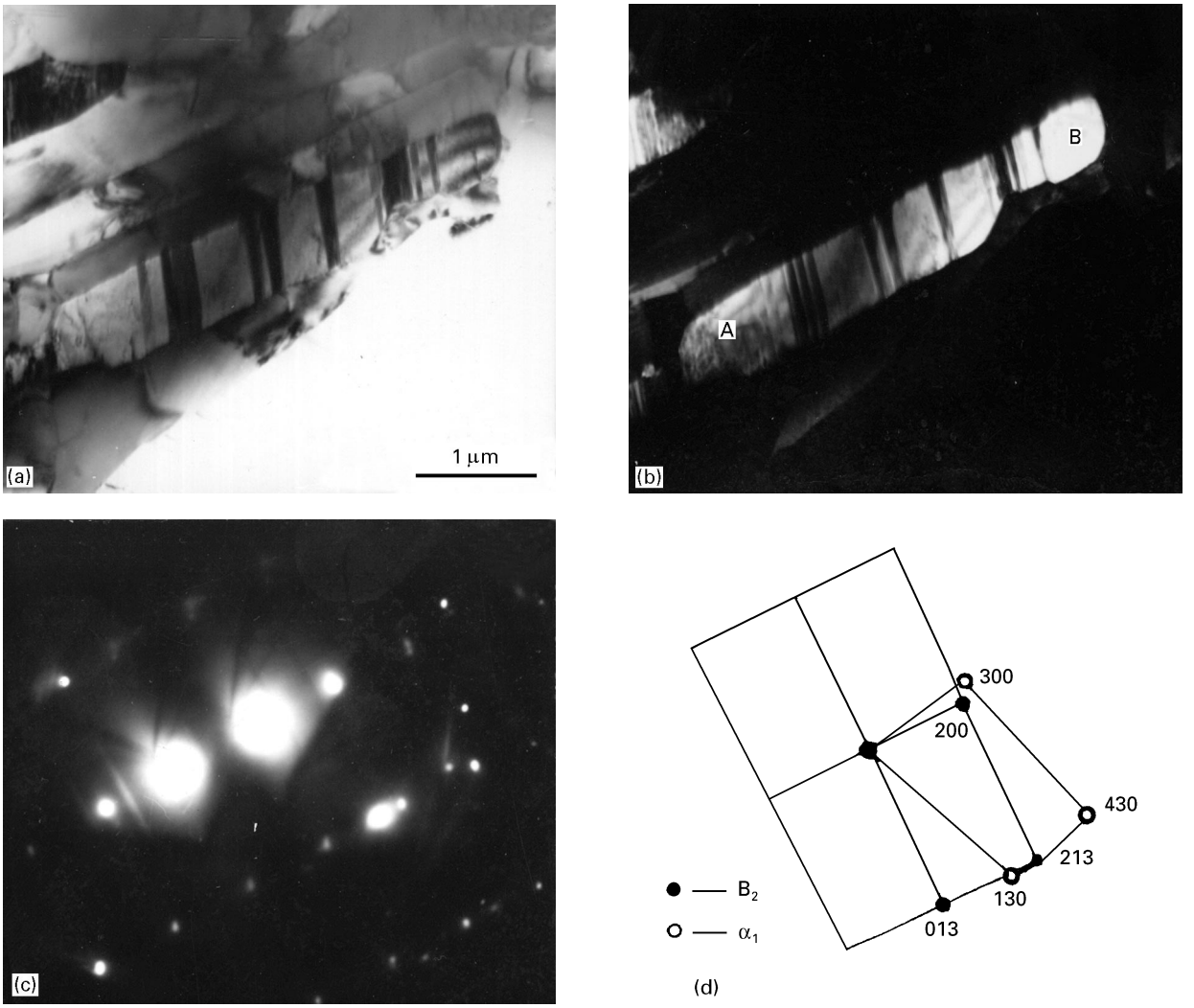

Figure 7 Subunits of bainite observed by TEM (305 °C; 45 s); (a) bright-field image; (b) dark-field image, $\mathbf{g} = 1\,3\,0_{\alpha_1}$; (c) selected-area diffraction pattern; (d) indexing result, ((●), B_2; (○), α_1) .

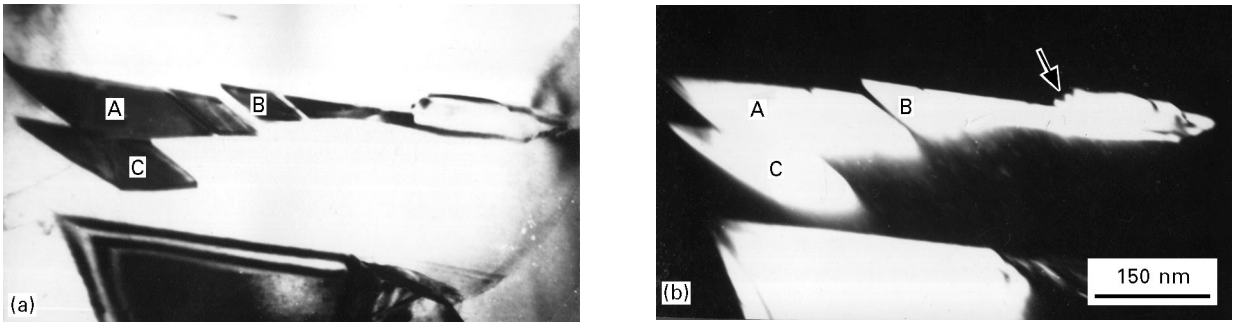

Figure 8 Subunits of bainite (250 °C; 6 min); (a) bright-field image; (b) dark-field image.

ledges exist on the broad faces and/or at the growth edges of α_1 plates [19, 20] which is consistent with the results reported by Chattopadhyay and Aaronson [18]. Also, evidences of mobility of ledges has been provided [20–22]. So, α_1 plates were considered to grow by the diffusion-controlled ledgewise mechanism [20].

In this alloy, the ledge structure of the α_1 plate was confirmed again. As illustrated in Fig. 9, the α_1 plate is free of stacking faults, and ledges are present on its two broad faces. Taking into account all the above experimental facts, it could be considered that, as a part of the bainite plate, the subunit also grows by a ledgewise mechanism.

3.3. Sympathetic nucleation of a subunit

If we suppose that bainite grown via the diffusion-controlled ledgewise mechanism, i.e., bainite lengthened and thickened by the lateral migration of risers on the broad faces of the plate, it would develop into a complete plate. Contrary to this assumption, however, the fact that bainite plate is composed of

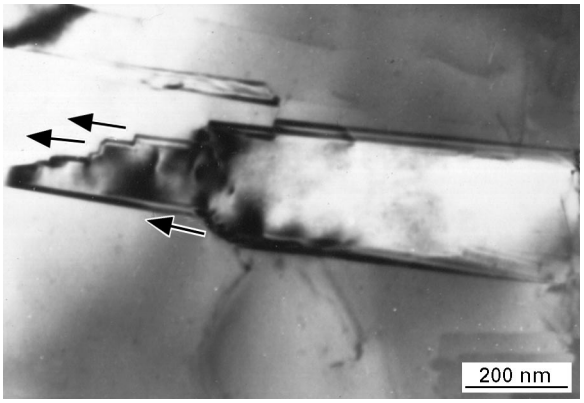

Figure 9 Ledge structure of a bainite plate (350 °C; 10 s).

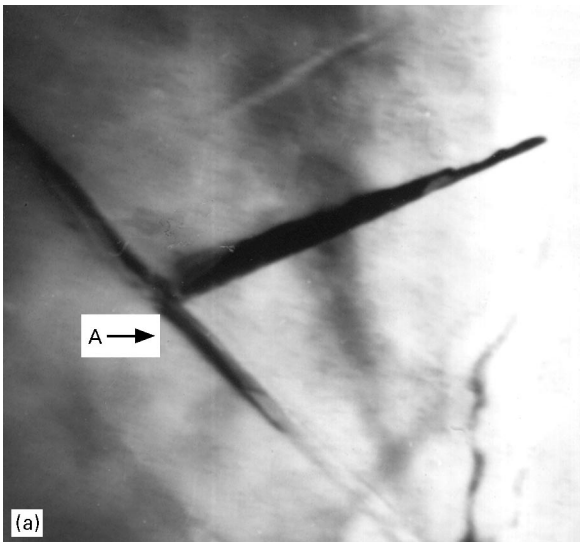

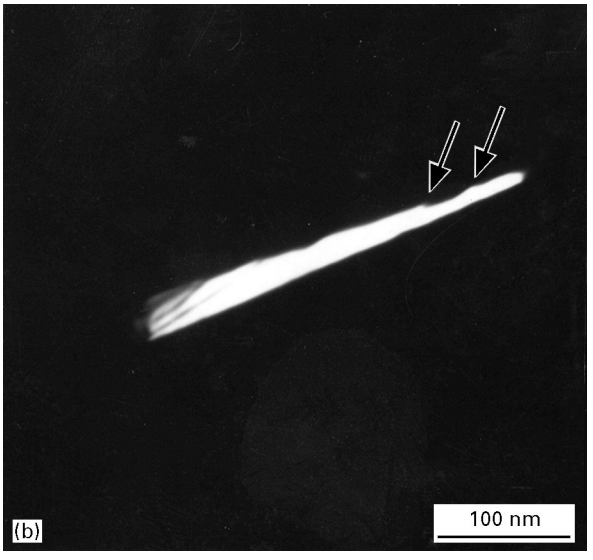

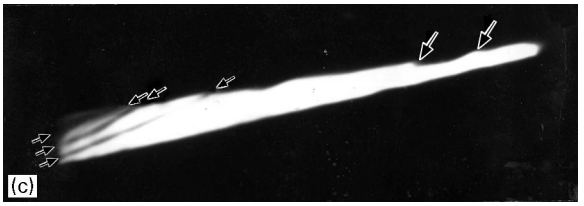

Figure 10 ETF and FTF sympathetic nucleation of subunits (250 °C; 6 min); (a) bright-field image; (b) dark-field image; (c) enlargement of (b).

subplates and subunits indicates that the α_1 plate does not always grow continuously by a ledgewise mechanism although the subunits grow in this manner. According to the experimental results described above, sympathetic nucleation is postulated here to account for the configuration of the α_1 plate.

The theory of sympathetic nucleation was first proposed by Aaronson and Well [23] and Street [24]. Subsequently, Unnikrishnan [25] made a thorough investigation. The theory is defined as the nucleation of a precipitated phase at the interphase boundary of the same pro-precipitated phase. The requirement of sympathetic nucleation is that a difference between the compositions of the matrix and precipitated phases exists and the precipitated phases are crystallographically correlated with each other. According to the morphology of precipitated phases, the sympathetic nucleation can be divided into three types: face to face (FTF), edge to edge (ETE) and edge to face (ETF), as shown in Fig. 3 of [26].

The sympathetic nucleation of α_1 plate in Cu–Zn–Al alloy is found to be similar to that of bainite in steel proposed in [26] and thus is not described here. Chattopadhyay and Aaronson [18] discovered this phenomenon in Cu–Zn alloys. In Fig. 1c of their paper, an α_1 plate is sympathetically nucleated at another plate and these two plates form the "Widmanstätten star" morphology.

In the present study, all the three types of sympathetic nucleaction of α_1 plate were also observed to occur. In Fig. 8a, all the subunits were nucleated sympathetically by ETE while subunits A and C are in the form of FTF. The situation of ETF sympathetic nucleation is shown in Fig. 10.

Fig. 10 is a micrograph of bainite with the specimen held at 250 °C for 6 min. It is easy to see that the bainite plates A and B belong to ETF sympathetic nucleation. In Fig. 10b, ledges exist at the tip of bainite plate B, as illustrated by the arrows. By careful inspection of the dark-field image in Fig. 10b, it can be discovered that bainite plate B is also made up of subunits. It reveals clearly that there are four subunits at the origin of plate B with their boundary indicated by the arrows. Obviously, all these subunits are formed sympathetically by FTF nucleation.

4. Discussion

4.1. The discovery of the subunit of the α_1 plate

As pointed out in [15], STM has a superior vertical resolution ability and thus can make up the corresponding deficit of SEM and TEM effectively. This makes it a powerful tool to reveal the surface microprofile of the specimen or, further, its fine structure. In the present study, the difference between the heights of two neighbouring subunits and the related boundary in Fig. 4 is about 10 nm, which far exceeds the spatial resolution of SEM or TEM in spite of their high lateral resolution of about 6 nm and 0.2 nm, respectively, and thus can hardly be distinguished by them. In contrast, this can be done easily by STM with the aid of its high lateral and vertical resolutions. This led to the discovery of subunit.

However, what we should point out is that the size of the subunit of the α_1 plate in the present alloy investigated here, 60 nm × 60 nm, is large enough, and that there exists a gap of about 10 nm (as shown in Fig. 4) between every two bounding subunits which can be distinguished by TEM; the real width of the gap is about one tenth of the corresponding result observed by STM as it is resulted from the etching procedure. For example, the matrix between two subunits in Fig. 7 and Fig. 8 is only 1–2 nm wide or even less than 1 nm in Fig. 10 as demonstrated by the arrows, which nearly reaches the experimental resolution limit of the TEM under normal imaging conditions. So it is not easy to distinguish the boundary between subunits by means of TEM. This was the reason for the failure of previous investigations to reveal the subunits of the bainite plate in Cu–Zn and Cu–Zn–Al alloys. However, the boundary between subunits can be widened and deepened through etching. For example, this gap can be widened from about 2 nm to about 10 nm. So, the subunits can be easily distinguished by STM and this led to their discovery.

On the other hand, it should also be noted that the STM study of subunits was carried out on the specimen surfaces revealed by chemical etching; so they could be interpreted as other structural defects such as the recovery of dislocations or other line defects and thus cannot provide any direct evidence for such processes. However, if the boundary between subunits resulted from structural defects, it should not be revealed by STM on the polished specimen surface. So, the present investigation dealing with fresh surface reliefs produced on a polished specimen heat treated in an ultrahigh vacuum together with the TEM study provide irrefutable experimental evidence of the existence of subunits.

4.2. Surface relief with bainite and martensite

The surface relief with bainite was first investigated by Ko and Cottrell [1]. They found that surface relief with bainite in steel is also of IPS type, i.e., identical with that associated with martensite. Ever since then, many experiments have been made, focusing on the surface relief with bainite and much disagreement remains. Surface relief with bainite (α_1 plates) in Cu–Zn alloys was also observed [5, 9]. These studies proposed that bainite transformed in the same way as martensite. As these previous studies introduced an optical interference microscope to investigate the surface relief, it is impossible to discover the fine interior structure of bainite because of its resolution limit (about 30 nm). For instance, the height difference between subplates in Fig. 6b is about 10 nm. Apparently, this cannot be distinguished by the optical interference microscope. Furthermore, the surface reliefs observed are actually groups of small reliefs and thus cannot provide the characteristics of transformation.

In this paper, we investigated the surface relief by means of STM. With a high lateral and vertical resolution as to ångström or even subångström level, it can provide perfectly the nature of surface relief and the fine structure of transformation products. The experiments demonstrate that the surface relief with bainite is composed of small reliefs, each corresponding to a subunit, which confirms the existence of subunits of bainite in Cu–Zn–Al alloy.

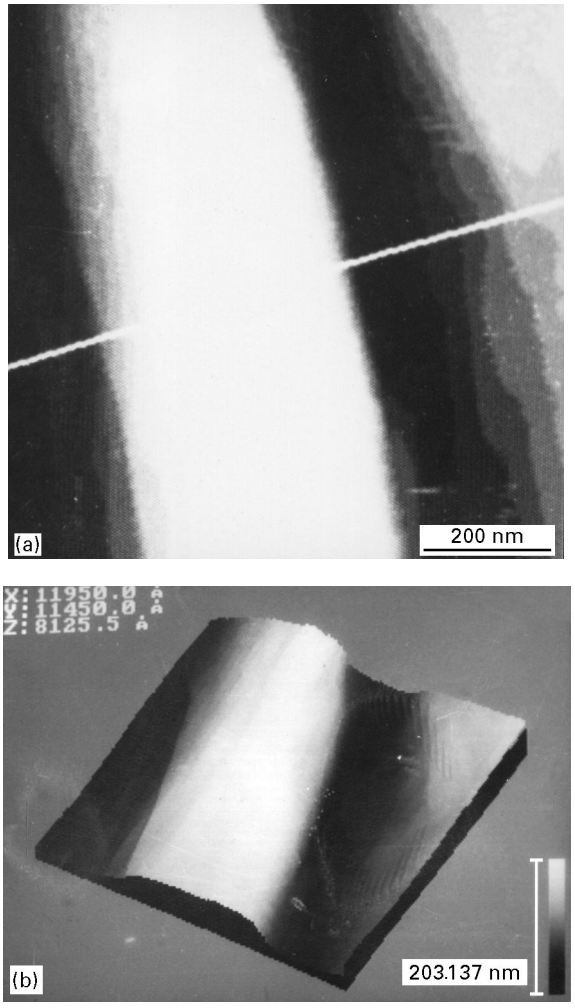

Figure 11 STM image of surface relief with martensite in Cu–Zn–Al alloy; (a) two-dimensional image; (b) three-dimensional image.

Apart from the surface relief with bainite, the surface relief accompanying martensite was also studied by STM. Fig. 11 shows the relief with a single martensite plate. It can be seen in Fig. 11a that the plate is about 0.8 μm wide. Contrary to the relief with bainite, the two sides of martensite is very smooth, and no subunit appears in this plate. The profile of this plate was also studied (as indicated by the white line in Fig. 11a) so as to allow comparison with that of bainite. It revealed that the shape of the surface relief is of typical IPS type, which means that it is transformed by a shear process. Fig. 11b is the three-dimensional image related to Fig. 11a.

4.3. Sympathetic ledgewise mechanism of α_1 plate

The experimental results given above illustrate that no shear characteristics accompany the formation of α_1 plate such as the absence of stacking faults which serve as the heterogeneity producing lattice-invariant deformation. Also, ledges had been exhibited on the

broad faces of the subunit at the α_1 plate tip which can be well interpreted by the ledgewise mechanism. Furthermore, if subunits formed in a given specimen upon bainitic reaction grow by a martensitic shear process, they would be of approximately the same size. Contrary to this assumption, however, the subunits shown in this paper differ significantly in size from each other with the maximum being about $1100\,nm \times 800\,nm$ while the minimum is $60\,nm \times 60\,nm$. In addition, the subunits were found to decrease progressively in size along their growth direction. Undoubtedly, the above proposal contradicts experiments. In contrast, according to all the results in this paper, a sympathetic nucleation–ledgewise growth mechanism occurs here in order to account for the behaviour of the α_1 plate. That is, subunits of bainite are sympathetically nucleated sequentially while each of them grows through a diffusion-controlled ledgewise mechanism.

Once α_1 plate forms via the diffusion-controlled lateral migration of a ledge in the matrix, the interface tends to be fully coherent during nucleation. In the course of growth, the strain energy associated with full coherency becomes too high and hence full coherency is usually replaced by partial coherency. Upon further ageing, the growth rate of the ledge of α_1 will decrease with increasing time because of the inadequacy of the driving force. At this time, another nucleus can form on the broad face at a ledge terrace after an incubation period. Energetically, the new nucleus will form on the dislocation line at the growth ledge terrace so as to obtain the extra driving force. The interface between the nucleus and the matrix, (as well as that between the nucleus and the α_1 plate) is usually semi-coherent so as to minimize the interfacial and strain energies. Consequently, the nucleus might form by FTF nucleation at the initial α_1–B2 boundary to consume boundary energy as much as possible. After it grows to a certain extent through the ledgewise mechanism, the growth of the new α_1 will also stop. If the condition is suitable, new α_1 will be formed by sympathetic nucleation. In this way, the nucleation process is repeated. As the process of sympathetic nucleation–ledgewise growth operates throughout the growth process of bainite, if all three types of sympathetic nucleation, i.e., FTF, ETF and ETE, operate simultaneously during bainite growing, a multilayer complex structure will be formed.

It is worth noting that, for a certain alloy and a given heat treatment, whether or not sympathetic nucleation accompanies ledgewise growth of bainite is determined by the reaction temperature and the alloy composition. For instance, bainite can develop extensively if the transformation occurs at a relatively high temperature; thus α_1 tends to take on a whole plate-like morphology. In contrast, if the isothermal temperature is low, a complicated structure i.e., the multilayer structure and subunits will form with α_1.

5. Conclusions

STM and TEM have been employed to reveal the fine structure and surface relief of bainite isothermally formed during ageing in a Cu–25.9 wt% Zn–4 wt% Al–0.1 wt% Re alloy. The results obtained are summarized as follows.

1. The bainite plates in the Cu–Zn–Al alloy are composed of subplates, and the subplates consist of subunits. Ledges of subunits were found to exist on the broad faces of the subplates.

2. The surface relief associated with bainite transformation is composed of groups of small reliefs which correspond to subplates and subunits. Only the nature of the surface relief accompanying a unique subunit can delineate the formation mechanism of bainite. It was found that the shape of the surface relief with a single subunit of bainite is tent like which is different from that with martensite. So it cannot be transformed by a shear mechanism.

3. Three types of sympathetic nucleation, FTF, ETE and ETF, were observed to operate in the formation of a subunit of the α_1 plate formed in this alloy.

4. All the experimental results show that α_1 plates are formed through a sympathetic nucleation–ledgewise growth mechanism.

Acknowledgements

This work was conducted under a grant from the National Natural Science Foundation of China, Beijing Electron Microscope Laboratory and Zhong Guancun Measurement and Analysis Fund of China. The authors would like to thank Professor H.I. Aaronson for his valuable suggestions on this paper during his invited lecture at the 1993 Chinese National Conference on Phase Transformations held in Beijing on 17–19 November 1993.

References

1. T. KO and S. A. COTTRELL, *J. Iron Steel Inst. London* **172** (1952) 307.
2. R. F. HEHEMANN, K. R. KINSMAN and H. I. AARONSON, *Metall Trans. A* **3** (1972) 1077.
3. H. K. D. H. BHADESHIA and D. V. EDMONDS, *Metall Trans A* **10** (1979) 895.
4. H. I. AARONSON, T. FURUHARA, J. M. RIGSBEE, W. T. REYNOLDS, Jr and J. M. HOWE, *Metall Trans. A* **21** (1990) 2369.
5. R. D. GARWOOD, *J. Inst. Metals.* **83** (1954–1955) 64.
6. *Idem.*, "Physical properties of martensite and bainites" (Iron and Steel Institute, London, 1965) pp. 90–127.
7. E. HORBOGEN and H. WARLIMONT, *Acta Metall.* **15** (1967) 943.
8. G. R. SRINIVASAN and M. T. HEPWORTH, *ibid.* **19** (1971) 1121.
9. I. CORNELIS and C. M. WAYMAN, *ibid.* **22** (1974) 301.
10. *Idem.*, *Scripta Metall.* **7** (1973) 579.
11. G. W. LORIMER, G. CLIFF, H. I. AARONSON and K. R. KINSMAN, *ibid.* **9** (1975) 1175.
12. P. DOIG and P. E. J. FLEWITT, *Mater. Sci.* **17** (1983) 601.
13. G. CLIFF, F. HASEN, G. W. LORIMER and M. KIKUCHI, *Metall Trans. A* **21** (1990) 831.
14. K. TAKEZAWA and S. SATO, *ibid.* **21** (1990) 1541.
15. G. BINNIG and H. ROHRER, *Helv. Phys. Acta.* **55** (1982) 726.
16. C.-L. BAI, "Scanning tunneling microscopy and applications" (Shanghai Science and Technology Press, Shanghai, 1992), pp. 10–11 (in Chinese).
17. H.-S. FANG, J.-J. WANG, Z.-G. YANG, C.-M. LI, X.-R. DENG, Y.-K. ZHENG, J.-J. YAN, H.-B. YU, Z.-G. LI and G. HUANG, Prog. Natural Sci. **4** (1994) 182.
18. K. CHATTOPADHYAY and H. I. AARONSON, *Acta Metall.* **34** (1986) 695.

19. C.-M. LI and H.-S. FANG, *Chin. Sci. Bull.* **39** (1994) 1435.
20. H.-S. FANG and C.-M. LI, *Metall. Mater. Trans. A* **25** (1994) 2615.
21. C.-M. LI and H.-S. FANG, *Prog. Natural Sci.* **4** (1994) 751.
22. C.-M. LI, H.-S. FANG, J.-J. WANG and Y.-K. ZHENG, *Mater. Lett.* **22** (1995) 233.
23. H. I. AARONSON and C. WELL, *Trans. AIME* **206** (1956) 1216.
24. J. A. STREET, *J. Inst. Metals* **88** (1959) 381.
25. M. UNNIKRISHNAN, *J. Mater. Sci.* **13** (1978) 1401.
26. H. S. FANG and J. J. WANG, *Acta Metall. Sin. A* **30** (1994) 491.

Received 19 April 1996
and accepted 29 July 1997